Magnetic field dependence of the spin fluctuations in $CeCu_{5.8}Ag_{0.2}$

X. Boraley [1], A. D. Christianson [2,*], J. Lass [1], C. Balz [3,4], M. Bartkowiak [1], Ch. Niedermayer [1], J. M. Lawrence [5], L. Poudel [4,6], D. G. Mandrus [6,7,8], F. Ronning [5], M. Janoschek [1,9] and D. G. Mazzone [1,†]

[1] *PSI Center for Neutron and Muon Sciences, 5232 Villigen PSI, Switzerland*

[2] *Materials Science and Technology Division, Oak Ridge National Laboratory, Oak Ridge, Tennessee 37831, USA*

[3] *ISIS Neutron and Muon Source, STFC Rutherford Appleton Laboratory, Didcot OX11 0QX, United Kingdom*

[4] *Neutron Scattering Division, Oak Ridge National Laboratory, Oak Ridge, Tennessee 37831, USA*

[5] *Los Alamos National Laboratory, Los Alamos, New Mexico, 87545, USA*

[6] *Department of Physics & Astronomy, University of Tennessee, Knoxville, Tennessee 37996, USA*

[7] *Materials Science & Technology Division, Oak Ridge National Laboratory, Oak Ridge, Tennessee 37831, USA*

[8] *Department of Materials Science & Engineering, University of Tennessee, Knoxville, Tennessee 37996, USA*

[9] *Physik-Institut, Universität Zurich, Winterthurerstrasse 190, CH-8057 Zurich, Switzerland*

(Received 15 September 2025; accepted 12 December 2025; published 28 January 2026)

Quantum phase transitions are among the most intriguing phenomena that can occur when the electronic ground state of correlated metals are tuned by external parameters such as pressure, magnetic field, or chemical substitution. Such transitions between distinct states of matter are driven by quantum fluctuations, and can give rise to macroscopically coherent phases that are at the forefront of condensed matter research. However, the nature of the critical fluctuations, and thus the fundamental physics controlling many quantum phase transitions, remain poorly understood in numerous strongly correlated metals. Here we study the model material $CeCu_{5.8}Ag_{0.2}$ to gain insight into the implications of critical fluctuations originating from different regions in reciprocal space. By employing an external magnetic field along the crystallographic *a* and *c* axis as auxiliary tuning parameter, we observe a pronounced anisotropy in the suppression of the quantum critical fluctuations, reflecting the spin anisotropy of the long-range ordered ground state at larger silver concentration. Coupled with the temperature dependence of the quantum fluctuations, these results suggest that the quantum phase transition in $CeCu_{5.8}Ag_{0.2}$ is driven by three-dimensional spin-density wave fluctuations.

DOI: 10.1103/bjgt-p16s

I. INTRODUCTION

A thermodynamic system of interacting particles assumes a variety of states of matter ranging from different configurations in solids to liquids, gases, and plasmas. Transformations between configurations occur as external conditions change, such as a solid that melts into a liquid at elevated temperature. Here we focus on continuous processes or phase transitions that can be driven either by thermal or quantum fluctuations. The latter fluctuations are particularly interesting, because they can trigger novel coherent states in solids that are potentially appealing for future technological applications [1–4]. Quantum phase transitions (QPTs) are governed by Heisenberg's uncertainty principle, conceptually distinguishing them from classical transitions. Quantum critical fluctuations diverge in space and imaginary time [5,6], elevating the effective dimension of the dynamic properties around the transition. These higher-dimensional fluctuations substantially alter the material properties around the QPT as has been shown by macroscopic resistivity, heat capacity, susceptibility, Grüneisen measurements, or through inelastic neutron scattering [7–11]. Their comparison to theoretical models allows for a detailed assessment of the quantum critical nature of the fluctuations [1,12–18]. However, in many metals the experimental observations disagree with the prevailing theoretical predictions of quantum fluctuations [19–24].

A central challenge in metals is that multiple degrees of freedom such as spin, charge, and lattice may become quantum critical. Long-range magnetic order is predominantly mediated via the RKKY interaction [25–27], in which the conduction electrons act as the exchange pathway between the localized ions. The prevailing theory derived by Hertz, Millis, and Moriya (HMM) predicts five dimensional quantum critical fluctuations for such a spin-density wave (SDW) quantum critical point [12–14], yielding mean-field behavior even close to the phase transition. Experimental realizations of SDW QPTs have been found in $Ce_{1-x}La_xRu_2Si_2$ and in $CeCu_2Ge_2$ under magnetic field, for instance [9,11]. However, in materials containing Ce, Yb, Sm, U, and other rare earths, the conduction electrons can also screen the local

*Contact author: christiansad@ornl.gov
†Contact author: daniel.mazzone@psi.ch

Published by the American Physical Society under the terms of the Creative Commons Attribution 4.0 International license. Further distribution of this work must maintain attribution to the author(s) and the published article's title, journal citation, and DOI.

moments via the Kondo effect [28]. A QPT associated with a quantum critical Kondo breakdown leads to local quantum critical fluctuations [15,16], which are thought to be at play in $CeRhIn_5$ [29], for instance. The interplay between the RKKY and Kondo interactions ultimately yields complex phase diagrams in which both effects can become quantum critical under extrinsic tuning parameters such as pressure, magnetic field, or chemical substitution [30,31]. Thus, accurate classifications of quantum criticality in rare-earth metals often require microscopic probes that can disentangle the contributions arising from long-range or local interactions, respectively.

Inelastic neutron scattering is a momentum-$\mathbf{Q}$ and energy-E resolved technique with a cross section that is proportional to the imaginary part of the dynamic susceptibility $\chi''(\mathbf{Q}, E)$. This enables precise separation of quantum fluctuations arising from different locations in reciprocal space. This has been particularly important to shed new light on a long-standing conundrum in the community [19–21,32,33]. Notably, the material $CeCu_6$ hosts quantum fluctuations around two different wave vectors $\mathbf{Q_1}$ and $\mathbf{Q_2}$ [34], and becomes quantum critical under 10% Au and 20% Ag substitution on the Cu site [19–21,32,33]. Pioneering inelastic neutron scattering experiments provided evidence for the existence of anomalous quantum critical fluctuations in $CeCu_{5.9}Au_{0.1}$ [19,20]. At larger Au (>10%) and Ag (>20%) concentration, members of the series establish magnetic long-range order that is suppressed in a SDW QPT under magnetic field [21,33,35]. A new prospective of this behavior was provided through a recent study on the zero-filed QPT of $CeCu_{5.8}Ag_{0.2}$ that profited from the latest generation of neutron spectrometers [32]. This study investigated a large $(\mathbf{Q}, E)$ volume with high momentum and energy resolution along with sufficient statistics to distinguish fluctuations from $\mathbf{Q_1} = (0.65, 0, 0.3)$ and $\mathbf{Q_2} = (1, 0, 0)$ in reciprocal lattice units (rlu). The experimental results revealed distinct behavior for the quantum fluctuations at $\mathbf{Q_1}$ and $\mathbf{Q_2}$. Notably, the authors noticed that the fluctuations at $\mathbf{Q_2}$ exhibit a small gap, but that the ones at $\mathbf{Q_1}$ condense into the elastic line and become quasielastic. The latter fluctuations also revealed a successive increase of the fluctuation life time with decreasing temperature, signifying critical slowing down of the quantum fluctuations which is a fingerprint of divergent imaginary time fluctuations around quantum critical points. Moreover, the dynamic properties at finite temperature provided evidence that the QPT in paramagnetic $CeCu_{5.8}Ag_{0.2}$ is also driven by SDW fluctuations [32].

In this article, we explore these recent insights by addressing the question of how external magnetic field affects the fluctuations in $CeCu_{5.8}Ag_{0.2}$ at $\mathbf{Q_1}$ and $\mathbf{Q_2}$. This is motivated by earlier studies of $CeCu_6$ showing a pronounced anisotropy in the magnetic susceptibility as a function of the magnetic field direction [36] and suppression of the magnetic excitations at moderate fields along the crystallographic c axis [34]. Further macroscopic studies of $CeCu_{6-x}Au_x$ and $CeCu_{6-x}Ag_x$ have identified the c axis as the easy axis and the b axis as the hardest axis in the series [36–38]. Our microscopic studies of $CeCu_{5.8}Ag_{0.2}$ reveal that the quantum critical fluctuations are sensitive to magnetic fields along the c axis, but remain unchanged at least up to $\mu_0 H = 8$ T for $H||b$. The result reflects the spin anisotropy of the long-range ordered ground state at larger Ag substitution [35], therefore supporting that the quantum critical fluctuations in $CeCu_{5.8}Ag_{0.2}$ arise from a SDW QPT.

II. EXPERIMENTAL DETAILS

Our study was conducted on the same well-characterized $CeCu_{5.8}Ag_{0.2}$ single crystal as used in Ref. [32] with $a = 8.173$, $b = 5.098$, and $c = 10.243$ Å. Two neutron spectrometers were used—(i) LET at the ISIS Neutron and Muons Source, United Kingdom [39], and (ii) CAMEA at the Paul Scherrer Institute (PSI), Switzerland [40,41] to map large reciprocal space regions for $H||b$ and c. The time-of-flight instrument LET was operated with 280 Hz and high-flux slits at the Resolution Chopper and 140 Hz at the Pulse Remover Chopper to produce neutrons with an incident energy $E_i = 3.7$ meV, yielding a resolution of 70 μeV at the elastic line. The sample was oriented with the c-axis vertical and cooled to a temperature $T = 250$ mK using a dilution insert in a vertical 9 T cryomagnet. Three-dimensional reciprocal-space maps were recorded with 1° sample rotation steps, and chosen such that $\mathbf{Q_1}$ and $\mathbf{Q_2}$ were accessible in the large area detector, taking advantage of the out-of-plane detector coverage the instrument provides. The background was measured at a field $\mu_0 H = 5$ T and $T = 250$ mK. The dynamic susceptibility tensor $\chi''(\mathbf{Q}, E)$ was derived from the measured dynamical structure factor $S(\mathbf{Q}, E)$ through $\chi''(\mathbf{Q}, E) \propto (1 - e^{-\frac{E}{k_B T}}) S(\mathbf{Q}, E)$ [42]. The temperature dependence ($0.1 \leqslant T \leqslant 4$ K) of the critical fluctuations were measured with the multiplexing spectrometer CAMEA using a $\mu_0 H = 1.8$ T horizontal magnet with large opening windows and a dilution insert. Two-dimensional reciprocal maps were measured with 1° sample rotation steps and incident energies, E_i, of 3.5 and 4.5 meV selected with a double-focusing HOPG monochromator. This configuration collects excitations up to $E < 1.4$ meV at an energy resolution of 110 μeV at the elastic line. The background was recorded at zero field and $T = 45$ K. The field dependence along the b axis was studied with CAMEA using a dilution insert in a vertical 11 T cryomagnet. $(\mathbf{Q}, E)$ maps were acquired at $T = 50$ mK with the same configuration as described above and fields ranging from $\mu_0 H = 0$ to 8 T. The temperature dependence at $\mu_0 H = 8$ T was measured between $T = 0.175$ and 3.18 K.

III. RESULTS

The magnetic excitation spectrum measured at LET in zero field and $T = 250$ mK is shown in Note 1 in the Supplemental Material (SM) [43]. Figures 1(a) and 1(b) depict the background-subtracted imaginary part of the dynamic susceptibility $\chi''(\mathbf{Q}, E)$ at $\mathbf{Q_1} = (\pm 0.65, 0, \pm 0.3)$ and $\mathbf{Q_2} = (1, 0, 0)$ as function of energy transfer and for fields applied along the c axis ranging from $\mu_0 H = 0$ to 3 T at $T = 250$ mK. The $\mu_0 H = 5$ T dataset was used as background, as we found that the fluctuations are suppressed at this field (see Note 1 in the SM [43]). At each $\mathbf{Q}$ position we integrated over 0.04 rlu^2 in the $(H, 0, L)$ plane, 0.4 rlu along the $(0, K, 0)$ axis. The intensity at $\mathbf{Q_1}$ results from an average over the four equivalent $\mathbf{Q}$ positions to enhance statistics. The energy dependence is

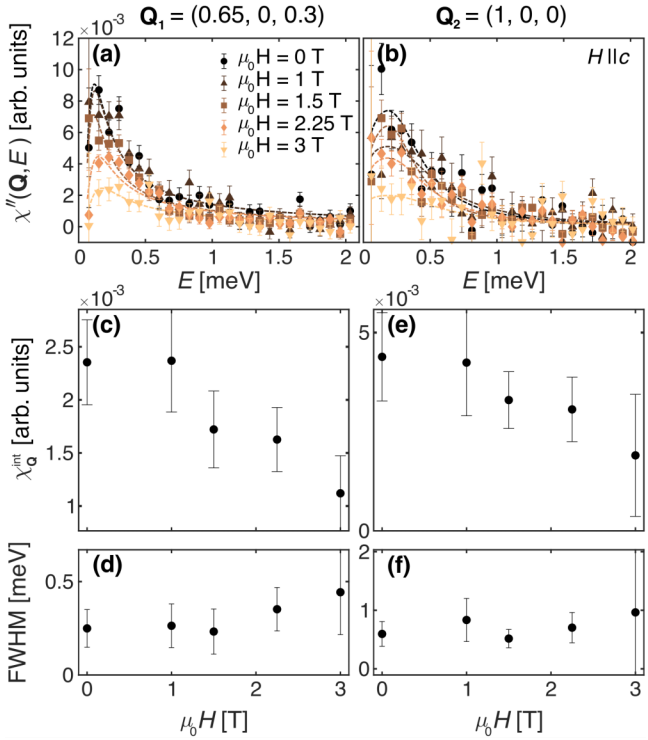


FIG. 1. Background-subtracted imaginary part of the dynamic susceptibility $\chi''(\mathbf{Q}, E)$ at (a) $\mathbf{Q_1} = (\pm 0.65, 0, \pm 0.3)$ in reciprocal lattice units (rlu) and (b) at $\mathbf{Q_2} = (1, 0, 0)$ as function of energy transfer E. The results were obtained at LET. Each data point was measured at $T = 250$ mK and integrated over 0.04 rlu^2 in the $(H, 0, L)$ plane, 0.4 rlu along the $(0, K, 0)$ axis, and over a 0.075 meV energy window. Spectra collected at $\mu_0 H = 5$ T were used as a background (see Note 1 in the SM [43] for details). (c)–(f) Integrated intensity $\chi^{\text{int}}_{\mathbf{Q}}$ and full-width at half-maximum (FWHM) extracted from modified quasielastic-Lorentzian fits at $\mathbf{Q_1}$ and Lorentzian fits at $\mathbf{Q_2}$ (see text for details).

modeled through a modified quasielastic Lorentzian

$$\chi''(\mathbf{Q}, E) = \frac{1}{\sqrt{3}} \frac{(E - E_0)\chi^{\text{int}}_{\mathbf{Q}}}{(E - E_0)^2 + \left(\frac{\Gamma}{2}\right)^2}, \tag{1}$$

which is normalized such that $\chi^{\text{int}}_{\mathbf{Q}}$ is the integrated intensity and the full-width at half maximum (FWHM) equals $\sqrt{3}\Gamma$. E_0 is an energy offset to test whether the excitation is indeed quasielastic. We obtained $E_0 = 49(9)$ μeV, which is within the elastic resolution of the instrument. The fit is shown as a dashed line in Fig. 1(a), and the resulting fitting parameters are reported in Figs. 1(c) and 1(d). A similar analysis is performed at $\mathbf{Q_2}$ using a Lorentzian

$$\chi''(\mathbf{Q}, E) = \frac{\frac{\Gamma}{4}\chi^{\text{int}}_{\mathbf{Q}}}{(E - E_0)^2 + (\frac{\Gamma}{2})^2}, \tag{2}$$

which is also normalized such that $\chi^{\text{int}}_{\mathbf{Q}}$ is the integrated intensity, the FWHM equals Γ, and $E_0 = 0.19(5)$ meV, reporting a gapped excitation. The field dependence of the parameters are reported in Figs. 1(e) and 1(f). We conclude that the quantum fluctuations in $CeCu_{5.8}Ag_{0.2}$ rapidly weaken for fields along the c axis and are suppressed at moderate fields of $\mu_0 H = 5$ T.

In all other experiments we collected large $(\mathbf{Q}, E)$ maps in the $(H, 0, L)$ plane at CAMEA to unambiguously separate the contributions of the fluctuations at $\mathbf{Q_1}$ and $\mathbf{Q_2}$. A representative energy slice integrated from $E = 0.15$–0.3 meV is shown in Fig. 2(a). The data is background subtracted and we removed Bragg-like signatures at $\mathbf{Q} = (-1, 0, \pm 1)$ and $\mathbf{Q_2}$ to highlight the broad fluctuations present in the material. The figure shows the fluctuations originating at $\mathbf{Q_1}$ and $\mathbf{Q_2}$ contribute both to energy cuts at specific $\mathbf{Q}$ points. Thus, we separated the two signals by the same approach as reported in Ref. [32]. The signal was parametrized with five two-dimensional Lorentzians of the form

$$y = \frac{A_{\mathbf{Q}}(E)}{1 + (\xi_{\parallel}^2 \cos^2\theta + \xi_{\perp}^2 \sin^2\theta)[(Q_H - Q_{H_i})^2 + (Q_L - Q_{L_i})^2]}, \tag{3}$$

where $y = \chi''(\mathbf{Q}, E)$, $A_{\mathbf{Q}}(E)$ is the signal amplitude, $\xi_{\parallel}$ and $\xi_{\perp}$ are the correlation lengths of the fluctuations, and θ is the angle between an arbitrary point $(Q_H, 0, Q_L)$ and $(Q_{H_i}, 0, Q_{L_i})$ which is $\mathbf{Q_1} = (\pm 0.65, 0, \pm 0.3)$ or $\mathbf{Q_2} = (1, 0, 0)$ (see Note 2 in the SM [43] for details). Cross correlations effects between different fitting parameters were minimized through an iterative fitting procedure. Notably the reference angle θ_0 required to define the orientation of $\xi_{\parallel}$ and $\xi_{\perp}$ (see Note 2 in the SM [43]) was found using a large energy window. All four correlation lengths were then fixed to their mean values resulting in $\xi_{\parallel} = 30(7)$ Å and $\xi_{\perp} = 46(7)$ Å at $\mathbf{Q_1}$, and along the crystallographic a and c axes $\xi_a = 23(4)$ Å and $\xi_c = 12(3)$ Å, respectively, at $\mathbf{Q_2}$. After this procedure the amplitudes at $\mathbf{Q_1}$ and $\mathbf{Q_2}$ were fitted, leading to the corresponding model shown in Fig. 2(b) alongside the individual $\mathbf{Q_1}$ and $\mathbf{Q_2}$ contributions in Figs. 2(c) and 2(d).

The field dependence of the fluctuations at $\mathbf{Q_1}$ and $\mathbf{Q_2}$ for $H||b$ and $T = 50$ mK is shown in Figs. 3(a) and 3(b), respectively. Consistent with the results reported in Ref. [32], we observe that the fluctuations at $\mathbf{Q_1}$ are quasielastic at zero magnetic field whereas at $\mathbf{Q_2}$ the fluctuations are gapped (see also Note 3 in the SM [43]). However, in contrast to the results obtained for $H||c$ we find that a magnetic field up to $\mu_0 H = 8$ T has no effect on the quantum fluctuations for $H||b$, suggesting a field anisotropy of the quantum fluctuations in the material. This anisotropy of the fluctuations was further studied through their temperature dependence at $\mu_0 H = 8$ T for $H||b$ and $\mu_0 H = 1.8$ T for $H||c$. The corresponding results are shown in Figs. 3(c) and 3(d) and Figs. 3(e) and 3(f), respectively. We find that the fluctuations at $\mathbf{Q_1}$ increase in intensity and become longer lived as the temperature decreases, suggesting a quantum critical slowing down of the fluctuations (see also Note 3 in the SM [43]). This is not observed for the fluctuations at $\mathbf{Q_2}$, which increase in intensity and move to lower energy transfers for $H||b$ as the temperature is decreased (further details are reported in Note 3 in the SM [43]). The different behavior of the quantum fluctuations at $\mathbf{Q_1}$ and $\mathbf{Q_2}$ as function of temperature provides evidence that the quantum critical fluctuations in $CeCu_{5.8}Ag_{0.2}$ originate from fluctuations at $\mathbf{Q_1}$.

The temperature dependence of the critical fluctuations at $\mathbf{Q_1}$ allows us to assess their nature through an analysis of their scaling behavior as function of E/T. This is possible because the higher-dimensional fluctuations close to QPTs

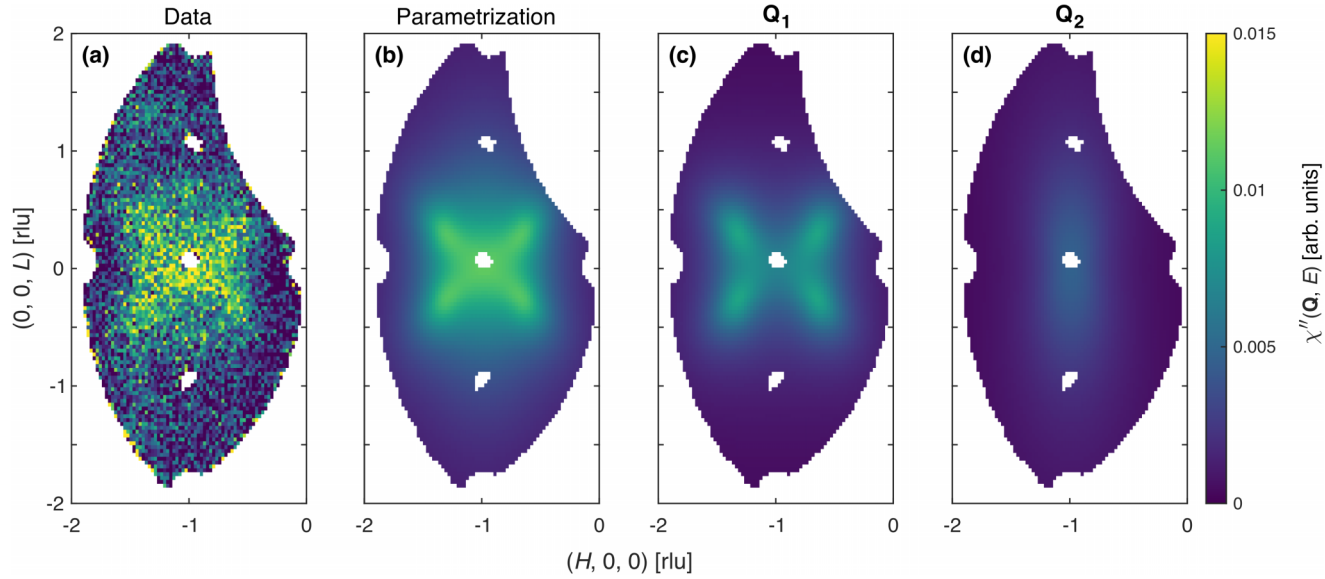


FIG. 2. (a) Background-subtracted constant energy slice (E integrated from 0.15 to 0.3 meV) in the $(H, 0, L)$ plane measured at $T = 50$ mK with CAMEA. (b)–(d) Parametrization of the experimental data using a combination of two-dimensional Lorentzians for the fluctuations at $\mathbf{Q_1} = (\pm 0.65, 0, \pm 0.3)$ and $\mathbf{Q_2} = (1, 0, 0)$ (see text for details).

yield scaling properties $\chi''(\mathbf{Q}, E) \cdot T^{\alpha} = f(\mathbf{Q}, E/T^{\beta})$ of universality classes specific to the nature of the quantum fluctuations. Notably, $\alpha = \beta = 1.5$ and $f(x) = abx/[1 + (bx)^2]$ is expected for a SDW quantum critical point (HMM model) [12–14,19,20,33], but $\alpha = 0.72$–0.83, $\beta = 1$, and $f(x) = c \sin(\alpha \arctan(x))/[(x^2 + 1)^{\alpha/2}]$ for a quantum critical Kondo breakdown (local model) [15,16,33,44–46]. We present the best fit to our data in Fig. 4, and report further details in Note 4 in the SM [43]. Our results show that the HMM model ($R^2 = 0.978$ for $H||b$ and $R^2 = 0.969$ for $H||c$) does a better job scaling the data than the local model ($R^2 = 0.878$ for $H||b$ and $R^2 = 0.865$ for $H||c$), and we refer to the next section for further discussions on the scaling behavior in $CeCu_{5.8}Ag_{0.2}$.

IV. DISCUSSION

The anisotropic field-dependent response of the quantum critical fluctuations provides new information about the nature of the QPT in $CeCu_{5.8}Ag_{0.2}$. The experimental data show

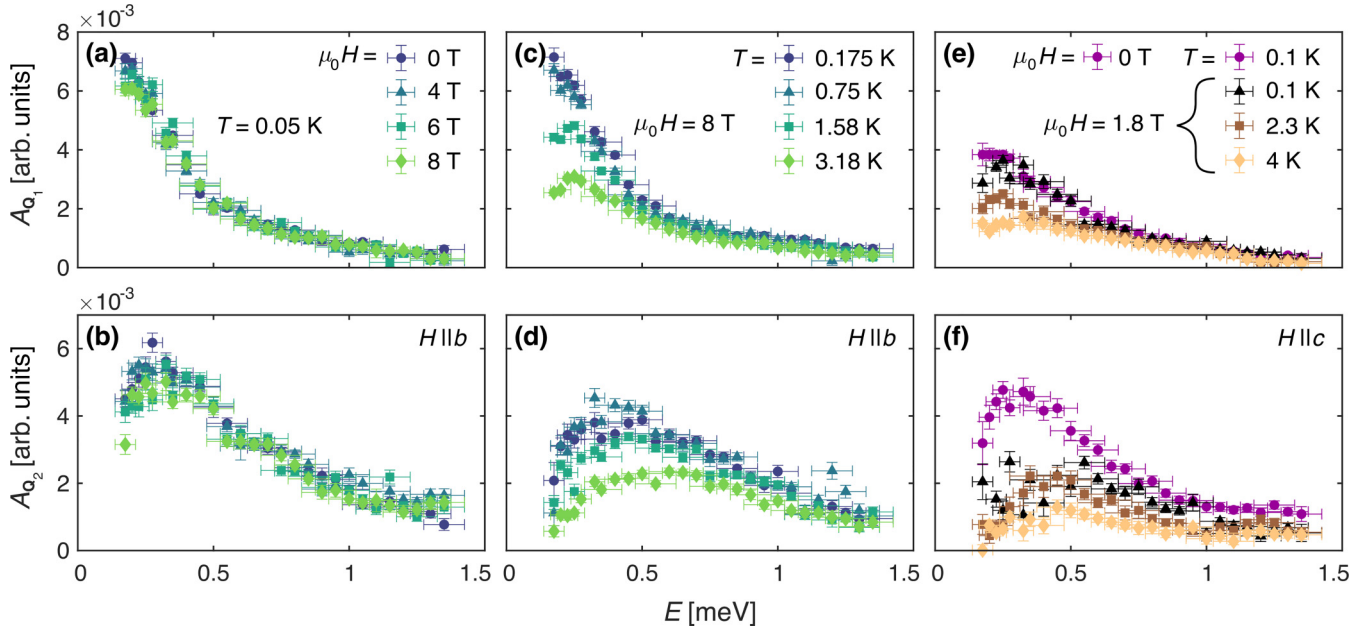


FIG. 3. Energy dependence of the fluctuation amplitude $A_{\mathbf{Q}}(E)$ at $\mathbf{Q_1} = (\pm 0.65, 0, \pm 0.3)$ [panels (a), (c), and (e)] and $\mathbf{Q_2} = (1, 0, 0)$ [panels (b), (d), and (f)] using the parametrization in Eq. (3). In panels (a) and (b) the magnetic field dependence of $A_{\mathbf{Q}}$ is shown for a field applied along the crystallographic b axis at $T = 50$ mK. (a) and (b) report the temperature dependence for a field of $\mu_0 H = 8$ T applied along the b axis. Panels (e) and (f) summarize the field and temperature dependence for a magnetic field along the the c axis.

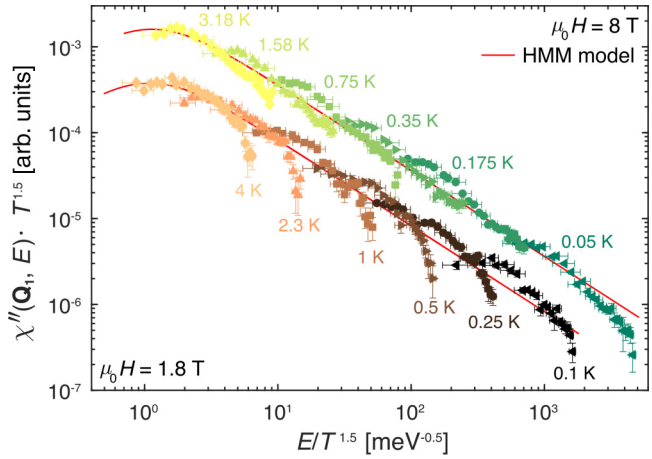


FIG. 4. Scaling analysis of the fluctuations centered at $\mathbf{Q_1} = (\pm 0.65, 0, \pm 0.3)$ using a HMM model with $\alpha = \beta = 1.5$. The upper dataset (yellow to green) was measured at $\mu_0 H = 8$ T along the b axis, for the lower dataset (orange to black) $\mu_0 H = 1.8$ T is applied along the c axis (the data points were vertically offset for clarity). The red lines represent the optimal fits to their respective data.

that the quantum fluctuations in the material are susceptible to magnetic fields aligned along the c axis, but remain unchanged at least up to $\mu_0 H = 8$ T for $H||b$. The result is in agreement with the magnetic field anisotropy of the magnetic long-range order at larger Ag concentrations and the magnetic susceptibility of the $CeCu_{6-x}Ag_x$ and $CeCu_{6-x}Au_x$ series, identifying the orthorhombic c and b direction as the soft and hard axis, respectively [36–38,47]. This suggests that the quantum critical fluctuations in $CeCu_{6-x}Ag_x$ with $x = 0.2$ are spin fluctuations connected to the long-range ordered magnetic moments at $x > 0.2$, which are amplitude modulated along the c axis [32]. Following this argument we hypothesize that the magnetic exchange couplings in $CeCu_{6-x}Ag_x$ are anisotropic and much weaker along the c axis when compared to the ones in the ab plane. While this would also be in line with the quasi-two-dimensional fluctuations that are thought to be relevant in the $CeCu_6$ family [48,49], it remains unclear how that anisotropy arises from the crystal-electric field scheme and the Fermi surface [50–53]. This encourages reinvestigations of the Fermi surface topology and neutron scattering experiments clarifying the ground state Hamiltonian of the $CeCu_6$ family, as they may help to further elucidate the connection of the quantum fluctuations with the spin degree of freedom.

Our analysis of the critical scaling behavior for $H||b$ at $\mu_0 H = 8$ T and $H||c$ at $\mu_0 H = 1.8$ T reveals that both datasets scale according to the HMM model with $R^2 = 0.978$ and 0.969, respectively. However, upon visual inspection of the results shown in Fig. 4, a better collapse of the data onto a single curve is observed for $H||b$ when compared to $H||c$. This suggests that the latter dataset is close to a conventional metallic regime in which HMM universality class is no longer valid (see also Note 6 in the SM [43] for detailed discussion). This statement is supported by macroscopic measurements of family members with larger Ag concentration, showing that regular Fermi liquid behavior is restored above $\mu_0 H \gtrapprox 2.3$ T for $CeCu_{5.2}Ag_{0.8}$ and $H||c$ [38,47]. This hypothesis can be tested with a study of the scaling behavior for $H||c$ at larger magnetic field strengths. However, technical challenges in neutron instrumentation restricts the feasibility of such experiments and may be achievable only in the future (see Note 5 in the SM [43] for further information). Additional studies on other $CeCu_{6-x}Ag_x$ and $CeCu_{6-x}Au_x$ family members may be also beneficial to clarify nature of the fluctuations at $\mathbf{Q_2}$ and why they shift with increasing temperature. We suspect that these fluctuations are related to Fermi surface effects.

Finally we argue that a decomposition of competing fluctuations into individual contributions via large ($\mathbf{Q}$, E) maps can be also advantageous in other cases. Many studies of metals containing rare-earth elements have reported results which are conflicting with prevailing theories of quantum fluctuations [22–24]. Here it is interesting to note that these studies have frequently focused on a few selected points in reciprocal space. In turn, those materials will benefit from a reinvestigation using state-of-the art neutron spectrometers. Moreover, the method may be also favorable to understand how quantum critical fluctuations are affected by magnetic frustration. Conceptually, it has been predicted that the complex phase diagrams spanned by the RKKY and Kondo interaction can be extended by magnetic frustration [1,16,54]. This has the potential to yield novel QPTs that produce unexplored phenomena such as metallic quantum spin liquid phases [7,55,56].

V. SUMMARY

The magnetic field dependence of the critical fluctuations in $CeCeu_{5.8}Ag_{0.2}$ was studied via inelastic neutron scattering. We find that the fluctuations are suppressed rapidly for fields aligned along the orthorhombic c axis, but remain robust up to at least $\mu_0 H = 8$ T for $H||b$. We separated the quantum fluctuations into two contributions at $\mathbf{Q_1} = (\pm 0.65, 0, \pm 0.3)$ and $\mathbf{Q_2} = (1, 0, 0)$, and observe that only the fluctuations at $\mathbf{Q_1}$ are quantum critical. Their temperature dependence at $\mu_0 H = 8$ and 1.8 T for $H||b$ and $H||c$, respectively, scales in accordance to the HMM model. Coupled with the observed anisotropy of the quantum critical fluctuations, the study suggests a SDW QPT in $CeCeu_{5.8}Ag_{0.2}$, reflecting the spin anisotropy of the long-range ordered state at larger Ag concentrations.

ACKNOWLEDGMENTS

We acknowledge the Paul Scherrer Institute and the ISIS Neutron and Muon Source for the allocated beam time on CAMEA and LET. We thank the Swiss National Science Foundation for financial support (Grant No. 200021_200653). The work by A.D.C. (contributions to project leadership, data interpretation, and manuscript preparation), D. G. Mandrus, and F.R. was supported by the U.S. Department of Energy, Office of Science, Basic Energy Sciences, Materials Sciences, and Engineering Division.

DATA AVAILABILITY

The data that support the findings of this article are openly available [57,58], embargo periods may apply.

[1] M. Vojta, Frustration and quantum criticality, Rep. Prog. Phys. **81**, 064501 (2018).

[2] L. Savary and L. Balents, Quantum spin liquids: A review, Rep. Prog. Phys. **80**, 016502 (2017).

[3] M. R. Norman, The challenge of unconventional superconductivity, Science **332**, 196 (2011).

[4] A. Narayan, A. Cano, A. V. Balatsky, and N. A. Spaldin, Multiferroic quantum criticality, Nat. Mater. **18**, 223 (2019).

[5] K. G. Wilson and J. Kogut, The renormalization group and the ϵ expansion, Phys. Rep. **12**, 75 (1974).

[6] S. Sachdev, *Quantum Phase Transitions*, 2nd ed. (Cambridge University Press, Cambridge, UK, 2011).

[7] Y. Tokiwa, C. Stingl, M.-S. Kim, T. Takabatake, and P. Gegenwart, Characteristic signatures of quantum criticality driven by geometrical frustration, Sci. Adv. **1**, e1500001 (2015).

[8] V. K. Anand, D. T. Adroja, A. D. Hillier, K. Shigetoh, T. Takabatake, J.-G. Park, K. A. McEwen, J. H. Pixley, and Q. Si, Zero-field ambient-pressure quantum criticality in the stoichiometric non-Fermi liquid system CeRhBi, J. Phys. Soc. Jpn. **87**, 064708 (2018).

[9] D. K. Singh, A. Thamizhavel, J. W. Lynn, S. Dhar, J. Rodriguez-Rivera, and T. Herman, Field-induced quantum fluctuations in the heavy fermion superconductor $CeCu_2Ge_2$, Sci. Rep. **1**, 117 (2011).

[10] V. H. Tran, A. D. Hillier, D. T. Adroja, and D. Kaczorowski, Antiferromagnetic spin fluctuations in the heavy-fermion superconductor Ce_2PdIn_8, Phys. Rev. B **86**, 094525 (2012).

[11] W. Knafo, S. Raymond, P. Lejay, and J. Flouquet, Antiferromagnetic criticality at a heavy-fermion quantum phase transition, Nat. Phys. **5**, 753 (2009).

[12] J. A. Hertz, Quantum critical phenomena, Phys. Rev. B **14**, 1165 (1976).

[13] A. J. Millis, Effect of a nonzero temperature on quantum critical points in itinerant fermion systems, Phys. Rev. B **48**, 7183 (1993).

[14] T. Moriya and T. Takimoto, Anomalous properties around magnetic instability in heavy electron systems, J. Phys. Soc. Jpn. **64**, 960 (1995).

[15] Q. Si, S. Rabello, K. Ingersent, and J. L. Smith, Locally critical quantum phase transitions in strongly correlated metals, Nature (London) **413**, 804 (2001).

[16] Q. Si and S. Paschen, Quantum phase transitions in heavy fermion metals and kondo insulators, physica Status Solidi (B) **250**, 425 (2013).

[17] S. Sachdev, Universal relaxational dynamics near two-dimensional quantum critical points, Phys. Rev. B **59**, 14054 (1999).

[18] T. R. Kirkpatrick and D. Belitz, Exponent relations at quantum phase transitions with applications to metallic quantum ferromagnets, Phys. Rev. B **91**, 214407 (2015).

[19] A. Schröder, G. Aeppli, E. Bucher, R. Ramazashvili, and P. Coleman, Scaling of magnetic fluctuations near a quantum phase transition, Phys. Rev. Lett. **80**, 5623 (1998).

[20] A. Schröder, G. Aeppli, R. Coldea, M. Adams, O. Stockert, H.v. Löhneysen, E. Bucher, R. Ramazashvili, and P. Coleman, Onset of antiferromagnetism in heavy-fermion metals, Nature (London) **407**, 351 (2000).

[21] H.v. Löhneysen, O. Stockert, and M. Enderle, Magnetic fluctuations at the field-tuned vs. concentration-tuned quantum phase transition in $CeCu_{6-x}Au_x$, J. Magn. Magn. Mater. **310**, 822 (2007), proceedings of the 17th International Conference on Magnetism.

[22] J.-G. Park, D. T. Adroja, K. A. McEwen, and A. P. Murani, Non-Fermi liquid behavior in the dynamic susceptibility of $Ce(Rh_{0.8}Pd_{0.2})Sb$, J. Phys.: Condens. Matter **14**, 3865 (2002).

[23] M. C. Aronson, R. Osborn, R. A. Robinson, J. W. Lynn, R. Chau, C. L. Seaman, and M. B. Maple, Non-Fermi-liquid scaling of the magnetic response in $UCu_{5-x}Pd_x (x = 1, 1.5)$, Phys. Rev. Lett. **75**, 725 (1995).

[24] C. Stock, C. Broholm, F. Demmel, J. Van Duijn, J. W. Taylor, H. J. Kang, R. Hu, and C. Petrovic, From incommensurate correlations to mesoscopic spin resonance in $YbRh_2Si_2$, Phys. Rev. Lett. **109**, 127201 (2012).

[25] M. A. Ruderman and C. Kittel, Indirect exchange coupling of nuclear magnetic moments by conduction electrons, Phys. Rev. **96**, 99 (1954).

[26] T. Kasuya, A theory of metallic ferro- and antiferromagnetism on Zener's model, Prog. Theor. Phys. **16**, 45 (1956).

[27] K. Yosida, Magnetic properties of Cu-Mn alloys, Phys. Rev. **106**, 893 (1957).

[28] J. Kondo, Resistance minimum in dilute magnetic alloys, Prog. Theor. Phys. **32**, 37 (1964),.

[29] H. Wang, T. B. Park, J. Kim, H. Jang, E. D. Bauer, J. D. Thompson, and T. Park, Evidence for charge delocalization crossover in the quantum critical superconductor $CeRhIn_5$, Nat. Commun. **14**, 7341 (2023).

[30] P. Coleman and A. J. Schofield, Quantum criticality, Nature (London) **433**, 226 (2005).

[31] S. Paschen and Q. Si, Quantum phases driven by strong correlations, Nat. Rev. Phys. **3**, 9 (2021).

[32] L. Poudel, J. M. Lawrence, L. S. Wu, G. Ehlers, Y. Qiu, A. F. May, F. Ronning, M. D. Lumsden, D. Mandrus, and A. D. Christianson, Multicomponent fluctuation spectrum at the quantum critical point in $CeCu_{6-x}Ag_x$, npj Quantum Mater. **4**, 52 (2019).

[33] O. Stockert, M. Enderle, and H. v. Löhneysen, Magnetic fluctuations at a field-induced quantum phase transition, Phys. Rev. Lett. **99**, 237203 (2007).

[34] J. Rossat-Mignod, L. P. Regnault, J. L. Jacoud, C. Vettier, P. Lejay, J. Flouquet, E. Walker, D. Jaccard, and A. Amato, Inelastic neutron scattering study of cerium heavy fermion compounds, J. Magn. Magn. Mater. **76-77**, 376 (1988).

[35] L. Poudel, C. de la Cruz, E. A. Payzant, A. F. May, M. Koehler, V. O. Garlea, A. E. Taylor, D. S. Parker, H. B. Cao, M. A. McGuire, W. Tian, M. Matsuda, H. Jeen, H. N. Lee, T. Hong, S. Calder, H. D. Zhou, M. D. Lumsden, V. Keppens, D. Mandrus, *et al.*, Structural and magnetic phase transitions in $CeCu_{6-x}T_x$ (T = Ag, Pd), Phys. Rev. B **92**, 214421 (2015).

[36] A. Amato, D. Jaccard, J. Flouquet, F. Lapierre, J. L. Tholence, R. A. Fisher, S. E. Lacy, J. A. Olsen, and N. E. Phillips, Thermodynamic and transport properties of $CeCu_6$, J. Low Temp. Phys. **68**, 371 (1987).

[37] H. G. Schlager, A. Schröder, M. Welsch, and H. v. Löhneysen, Magnetic ordering in $CeCu_{6-x}Au_x$ single crystals: Thermodynamic and transport properties, J. Low Temp. Phys. **90**, 181 (1993).

[38] E.-W. Scheidt, D. Maurer, A. Weber, T. Götzfried, K. Heuser, S. Kehrein, and R. Tidecks, Quantum phase transitions: Experimental facts—a challenge for theory, Phys. B: Condens. Matter **321**, 133 (2002), Proceedings of the Sec-

ond Regional Conference on Magnetic and Superconducting Materials.

[39] R. I. Bewley, J. W. Taylor, and S. M. Bennington, LET, a cold neutron multi-disk chopper spectrometer at ISIS, Nucl. Instrum. Methods Phys. Res. Sect. A **637**, 128 (2011).

[40] J. Lass, H. Jacobsen, K. M. L. Krighaar, D. Graf, F. Groitl, F. Herzog, M. Yamada, C. Kägi, R. A. Müller, R. Bürge, M. Schild, M. S. Lehmann, A. Bollhalder, P. Keller, M. Bartkowiak, U. Filges, U. Greuter, G. Theidel, H. M. Rønnow, Ch. Niedermayer, *et al.*, Commissioning of the novel continuous angle multi-energy analysis spectrometer at the Paul Scherrer Institut, Rev. Sci. Instrum. **94**, 023302 (2023),.

[41] J. Lass, H. Jacobsen, D. G. Mazzone, and K. Lefmann, MJOLNIR: A software package for multiplexing neutron spectrometers, SoftwareX **12**, 100600 (2020).

[42] A. Furrer, J. Mesot, and T. Strässle, *Neutron Scattering in Condensed Matter Physics* (World Scientific, 5 Toh Tuck Link, Singapore, 2009).

[43] See Supplemental Material at http://link.aps.org/supplemental/10.1103/bjgt-p16s for more detailed results and additional information on the data analysis, which also includes Refs. [59–61].

[44] M. T. Glossop and K. Ingersent, Magnetic quantum phase transition in an anisotropic Kondo lattice, Phys. Rev. Lett. **99**, 227203 (2007).

[45] D. R. Grempel and Q. Si, Locally critical point in an anisotropic Kondo lattice, Phys. Rev. Lett. **91**, 026401 (2003).

[46] J.-X. Zhu, S. Kirchner, R. Bulla, and Q. Si, Zero-temperature magnetic transition in an easy-axis Kondo lattice model, Phys. Rev. Lett. **99**, 227204 (2007).

[47] K. Heuser, J. S. Kim, E. W. Scheidt, T. Schreiner, and G. R. Stewart, Inducement of non-Fermi-liquid behavior with magnetic field in heavy-fermion antiferromagnets, Phys. B: Condens. Matter **259-261**, 392 (1999).

[48] R. Küchler, P. Gegenwart, K. Heuser, E.-W. Scheidt, G. R. Stewart, and F. Steglich, Grüneisen ratio divergence at the quantum critical point in $CeCu_{6-x}Ag_x$, Phys. Rev. Lett. **93**, 096402 (2004).

[49] H. v. Löhneysen, Fermi-liquid instability at magnetic–nonmagnetic quantum phase transitions, J. Magn. Magn. Mater. **200**, 532 (1999).

[50] U. Witte, O. Stockert, R. Schedler, L. P. Regnault, and M. Loewenhaupt, Crystalline electric field excitations in $CeCu_6$ studied by single crystal measurements with polarized neutrons, Phys. B: Condens. Matter **397**, 20 (2007).

[51] E. A. Goremychkin and R. Osborn, Neutron-spectroscopy study of the heavy-fermion compound $CeCu_6$, Phys. Rev. B **47**, 14580 (1993).

[52] S. Chapman, M. Hunt, P. Meeson, P. H. P. Reinders, M. Springford, and M. Norman, Heavy quasiparticles in $CeCu_6$ studied using magnetic quantum oscillations, J. Phys.: Condens. Matter **2**, 8123 (1990).

[53] H. Harima and A. Yanase, Fermi surfaces of $CeCu_6$ and $CeCu_2Si_2$, J. Magn. Magn. Mater. **108**, 145 (1992).

[54] P. Coleman and A. H. Nevidomskyy, Frustration and the Kondo effect in heavy fermion materials, J. Low Temp. Phys. **161**, 182 (2010).

[55] H. Zhao, J. Zhang, M. Lyu, S. Bachus, Y. Tokiwa, P. Gegenwart, S. Zhang, J. Cheng, Y.-f. Yang, G. Chen, Y. Isikawa, Q. Si, F. Steglich, and P. Sun, Quantum-critical phase from frustrated magnetism in a strongly correlated metal, Nat. Phys. **15**, 1261 (2019).

[56] Y. Tokiwa, M. Garst, P. Gegenwart, S. L. Bud'ko, and P. C. Canfield, Quantum bicriticality in the heavy-fermion metamagnet YbAgGe, Phys. Rev. Lett. **111**, 116401 (2013).

[57] D. G. Mazzone, M. Janoschek, C. Balz, Ch. Niedermayer, and X. Boraley, Understanding multicomponent quantum criticality in $CeCu_{5.8}Ag_{0.2}$, STFC ISIS Neutron and Muon Source, doi:10.5286/ISIS.E.RB2210367.

[58] X. Boraley, A. Christianson, J. Lass, C. Balz, M. Bartkowiak, Ch. Niedermayer, J. M. Lawrence, L. Poudel, D. Mandrus, F. Ronning, M. Janoschek, and D. G. Mazzone, Data for "Magnetic field dependence of critical fluctuations in $CeCu_{5.8}Ag_{0.2}$", Zenodo (2025), doi: 10.5281/zenodo.16939914.

[59] W. Knafo and S. Raymond, Artificial scaling laws of the dynamical magnetic susceptibility in heavy-fermion systems, Phys. Lett. A **341**, 251 (2005).

[60] O. Arnold, J. C. Bilheux, J. M. Borreguero, A. Buts, S. I. Campbell, L. Chapon, M. Doucet, N. Draper, R. Ferraz Leal, M. A. Gigg, V. E. Lynch, A. Markvardsen, D. J. Mikkelson, R. L. Mikkelson, R. Miller, K. Palmen, P. Parker, G. Passos, T. G. Perring, R. F. Peterson, *et al.*, Mantid—data analysis and visualization package for neutron scattering and μSR experiments, Nucl. Instrum. Methods Phys. Res. Sect. A **764**, 156 (2014).

[61] R. A. Ewings, A. Buts, M. D. Le, J. van Duijn, I. Bustinduy, and T. G. Perring, Horace: Software for the analysis of data from single crystal spectroscopy experiments at time-of-flight neutron instruments, Nucl. Instrum. Methods Phys. Res. Sect. A **834**, 132 (2016).